

---

# BIASED LOCAL SGD FOR EFFICIENT DEEP LEARNING ON HETEROGENEOUS SYSTEMS

---

**Jihyun Lim**  
Inha University  
wlguslim@inha.edu

**Junhyuk Jo**  
Inha University  
911whwnsgur@inha.edu

**Chanhyeok Ko**  
Mondrian AI  
chanhyeok@mondrian.ai

**Young Min Go**  
Mondrian AI  
ymgo@mondrian.ai

**Jimin Hwa**  
Mondrian AI  
hwa@mondrian.ai

**Sunwoo Lee**  
Inha University  
sunwool@inha.ac.kr

## ABSTRACT

Most large-scale neural network training methods assume homogeneous parallel computing resources. For example, synchronous SGD with data parallelism, the most widely used parallel training strategy, incurs significant synchronization overhead when workers process their assigned data at different speeds. Consequently, in systems with heterogeneous compute resources, users often rely solely on the fastest components, such as GPUs, for training. In this work, we explore how to effectively use heterogeneous resources for neural network training. We propose a system-aware local stochastic gradient descent (local SGD) method that allocates workloads to each compute resource in proportion to its compute capacity. To make better use of slower resources such as CPUs, we intentionally introduce bias into data sampling and model aggregation. Our study shows that well-controlled bias can significantly accelerate local SGD in heterogeneous environments, achieving comparable or even higher accuracy than synchronous SGD with data-parallelism within the same time budget. This fundamental parallelization strategy can be readily extended to diverse heterogeneous environments, including cloud platforms and multi-node high-performance computing clusters.

## 1 Introduction

Most large-scale neural network training methods assume homogeneous parallel computing resources. For example, synchronous SGD with data parallelism, the most widely used parallel training strategy, incurs significant synchronization overhead when workers process their assigned data at different speeds. Local SGD with periodic averaging, a foundational distributed optimization algorithm in federated learning, also suffers from the same limitation. While it reduces synchronization cost by decreasing the frequency of model aggregation, it still incurs substantial overhead at each aggregation point. Consequently, on modern GPU servers, relatively slower CPU resources often remain idle during training, even though CPUs are still powerful compute resources.

Some prior works have proposed deep learning methods designed to exploit heterogeneous system resources. BytePS dedicates CPUs to summation operations only while GPUs compute gradients [10]. HetSeq introduces bias into synchronous SGD with data-parallelism to more effectively utilize heterogeneous GPUs [6]. DistDGL also utilizes both CPUs and GPUs to train large-scale graph neural networks. FusionFlow is a load scheduler that uses CPUs to assist slower GPUs [13]. Metis is another load-balancing method designed for distributed training on heterogeneous GPUs [22]. While all these methods effectively utilize CPU resources to improve the efficiency of synchronous SGD, they commonly overlook the potential of using alternative distributed optimizers, such as local SGD. These methods also commonly introduce bias into gradient approximation, however, they do not investigate its impact.

In this study, we focus on how to utilize heterogeneous compute resources to efficiently train neural networks. Specifically, we develop a general parallel neural network training framework that minimizes synchronization costs across heterogeneous resources while achieving accuracy comparable to that of synchronous SGD with data-parallelism. To eliminate synchronization costs, we first adopt local stochastic gradient descent (local SGD) with periodic model

averaging. We propose a system-aware adjustment of the number of local updates within each communication round, allowing faster resources to perform more updates than slower ones. We then inject carefully controlled bias into local SGD to compensate for the fewer updates performed by slower resources.

The key principle behind our proposed framework is to inject bias into gradient estimation through data sampling and model aggregation. First, the framework monitors the training loss of each data sample and gives slow workers a higher probability of sampling high-loss data. This biased data sampling is expected to *improve the quality of local models trained on slow resources*, thereby accelerating the overall training process. Second, our framework adjusts the aggregation weights based on the number of local updates per communication round. As a result, *local models trained for more iterations more strongly contribute to global model training*. In this study, we demonstrate that these two independently introduced, system-aware biases enable more effective utilization of heterogeneous system resources compared to the conventional synchronous or local SGD.

To evaluate the performance of the proposed parallel neural network training framework, we perform representative deep learning benchmarks. Our extensive empirical study shows that our system-aware biased local SGD effectively utilizes not only fast GPUs but also relatively slower CPUs, achieving the highest accuracy within a fixed time budget. We conduct a comprehensive empirical study comparing several realistic heterogeneous settings, such as parallel neural network training using two CPUs and eight GPUs. The proposed framework is readily applicable to many realistic heterogeneous systems including cloud computing and multi-node high-performance platforms.

Our main contributions are summarized as follows.

- Our study explores a novel local SGD-based approach for efficient parallel neural network training on heterogeneous compute resources. We empirically prove that unbalanced local SGD is a suitable optimizer for deep learning in heterogeneous environments due to its efficiency and flexibility.
- We demonstrate that, across heterogeneous compute resources, the synchronization overhead of local SGD can be eliminated by system-aware adjustment of the number of local updates per round. This makes our method readily applicable to large-scale deep learning applications.
- We also show that introducing well-controlled bias into local SGD can dramatically accelerate parallel neural network training while matching the accuracy of synchronous SGD with data-parallelism.

## 2 Background

**Problem Definition** – In this work, we consider a minimization problem as follows.

$$F(\mathbf{W}) = \frac{1}{N} \sum_{i=1}^N f(\mathbf{W}, \xi_i), \quad (1)$$

where  $N$  is the number of data samples and  $f(\cdot, \cdot)$  is a loss function (e.g., cross entropy). Typically,  $f(\cdot)$  is a non-convex and smooth function such as neural networks.

**Local Stochastic Gradient Descent** – Local stochastic gradient descent (SGD) is a variant of SGD designed for communication-efficient model training. First it replicates the model to all workers. Then, each worker locally trains the received model using a numerical optimization algorithm such as mini-batch SGD. After a certain number of updates, the local models are averaged globally. These steps are called *communication round*. The update rule is written as follows.

$$\mathbf{W}^{t+1} = \mathbf{W}^t - \eta \frac{1}{P} \sum_{i=1}^P \sum_{j=0}^{\tau-1} \nabla f(\mathbf{W}_i^{t,j}) \quad (2)$$

Local SGD repeatedly runs communication rounds until the global model converges. In modern high-performance or large-scale cloud computing platforms, all individual workers can access the entire dataset thanks to parallel file systems. As a result, the dataset is IID, and thus  $\mathbb{E}[\nabla f_i(\mathbf{W})] = \nabla F(\mathbf{W})$ ,  $\forall i \in [P]$ .

**Biased Gradient Approximation** – To efficiently solve the minimization problem shown in (1), optimizers such as SGD approximate the first-order gradient of  $F(\cdot)$  using randomly sampled data. Instead of a single data point (or sample), a small batch of data is typically used to make a practical trade-off between system efficiency and stochastic efficiency. When the batch is sampled based on a uniform random distribution, the approximated gradient is unbiased such that  $\mathbb{E}[\nabla f(\mathbf{W}, \xi)] = \nabla F(\mathbf{W})$ . In this study, however, we break this convention and explore how introducing bias into the gradient approximation can accelerate parallel neural network training.

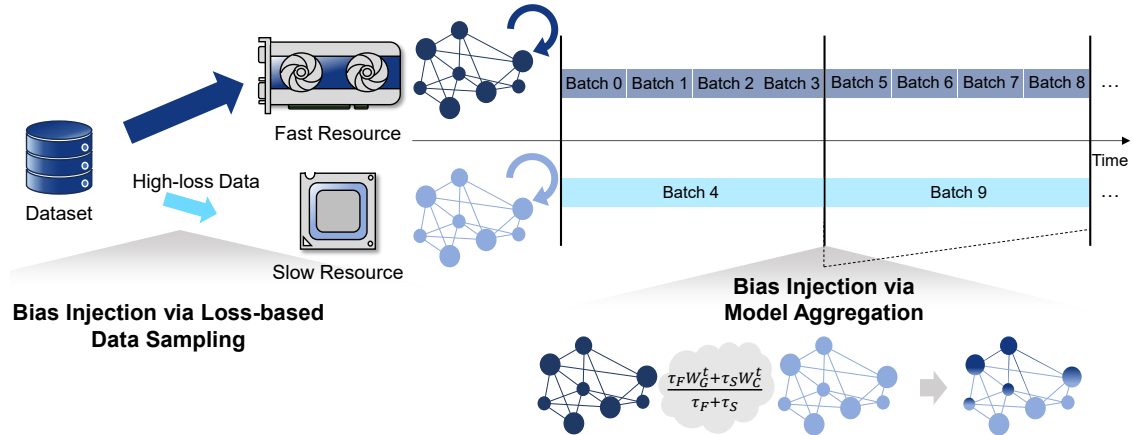


Figure 1: A schematic illustration of system-aware biased local SGD framework. The  $\tau_F$  and  $\tau_S$  are the number of local updates within each communication round on fast and slow resources, respectively. The  $W_G^t$  and  $W_C^t$  are the models locally updated on GPU and CPU, respectively.

### 3 Related work

**Local SGD under IID Settings** – Some prior works provide a theoretical foundation for local SGD under IID settings. [21, 8, 12]. Recently, STL-SGD has been proposed, which accelerates local SGD by adaptively adjusting model aggregation period [20]. While these previous works consider local SGD under IID settings, they either focus on theoretical performance guarantees or do not consider the system efficiency aspects.

**Biased Gradient Approximation** – Several prior works have explored the use of bias in deep learning. *Active Bias* is a training strategy that introduces bias toward high-variance samples [3]. *DIHCL* is a curriculum learning strategy that assigns higher weights to ‘hard-to-learn’ samples. An importance sampling method has also been proposed that estimates each sample’s significance using an approximated gradient norm bound [11]. More recently, a classification strategy based on the population stability index was introduced to address class-imbalanced problems [25]. Although these methods effectively leverage different forms of bias to accelerate training, they do not take into account the available system resources.

**Deep Learning on Heterogeneous Systems** – Several previous studies have proposed deep learning approaches tailored to exploit heterogeneous system resources. *BytePS* assigns CPUs exclusively to summation tasks, while GPUs are responsible for gradient computation [10]. *HetSeq* incorporates bias into synchronous SGD with data-parallelism to better utilize heterogeneous GPUs [6]. *DistDGL* uses CPUs and GPUs together to train large-scale graph neural networks efficiently. *FusionFlow* acts as a load scheduler, assigning auxiliary tasks to CPUs to support slower GPUs [13]. *Metis* is another load-balancing framework designed for distributed training across heterogeneous GPUs [22]. Although these methods effectively exploit CPU resources to accelerate synchronous SGD, they tend to overlook the potential of alternative distributed optimizers, such as local SGD. These methods also inherently introduce bias into gradient approximation, however, they do not consider its impact.

All these prior works either focus on biased gradient approximation without considering the underlying system resources, or on parallel training schemes that overlook the inherent bias they introduce. In this study, we explore how system-aware bias can be exploited to better utilize heterogeneous resources for fast and accurate large-scale deep learning.

### 4 Method

In this section, we first introduce a local SGD-based neural network training framework designed to leverage heterogeneous system resources. We then present two bias injection techniques and describe how they are integrated into the proposed framework.

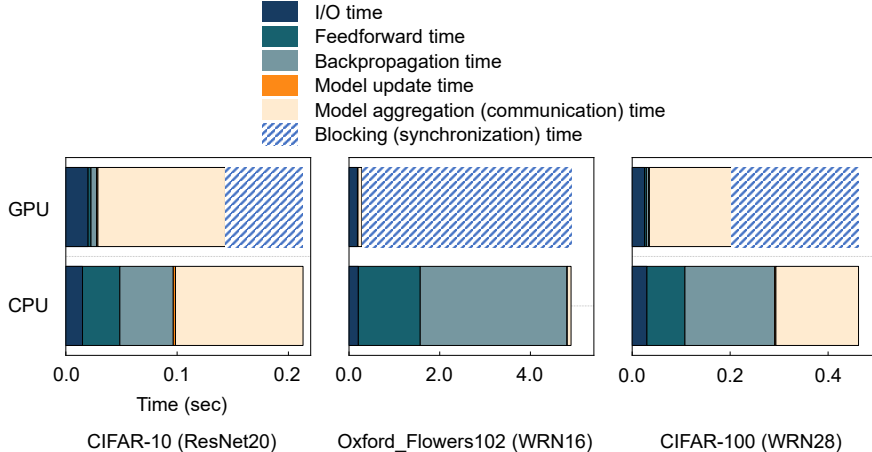


Figure 2: Timing breakdown of a single training step, measured on an AMD EPYC 7543 CPU and an NVIDIA GeForce RTX 4090 GPU. CPU training is an order of magnitude slower than GPU training. The resulting timing gap causes GPUs to remain idle, representing the synchronization cost.

#### 4.1 Local SGD on Heterogeneous Resources

**Motivation** – We begin by discussing potential challenges in utilizing relatively slow compute resources, such as CPUs, for parallel neural network training. The most common parallelization strategy is synchronous SGD with data parallelism. However, modern GPU servers often contain heterogeneous compute resources, including CPUs and GPUs with varying compute capabilities. In such systems, synchronous SGD and balanced local SGD, where all workers perform the same number of local updates per communication round, incur high synchronization costs, as faster workers must wait for slower ones to reach the synchronization point (e.g., model aggregation).

Figure 2 shows the timing breakdown of neural network training on a GPU server equipped with an AMD EPYC 7543 CPU and an NVIDIA GeForce RTX 4090 GPU. Across all datasets, synchronous SGD consistently suffers from substantial GPU blocking time. In particular, the Oxford Flowers 102 dataset contains relatively larger images than the CIFAR datasets, resulting in a significant computational efficiency gap between the CPU and GPU. When local SGD is applied, the total number of model aggregations is reduced, thereby lowering synchronization costs. However, the idle time of faster workers per aggregation remains unchanged. As the performance gap between compute resources widens, this overhead will be increasingly significant. This observation motivates us to explore a novel local SGD-based parallel neural network training framework that explicitly addresses synchronization overhead.

**Unbalanced Local SGD Framework** – We begin with proposing a general framework of local SGD-based parallel neural network training. To eliminate the synchronization cost caused by the performance gap across compute resources, we design a system-aware unbalanced local SGD. Specifically, a worker utilizing faster resources performs more local updates than one using slower resources. Figure 1 shows a schematic illustration of our framework.

We define two notations:  $\tau_S$  and  $\tau_F$ , representing the number of local updates per communication round on slow and fast resources, respectively. Note that, for simplicity, we only consider two types of system resources: fast and slow. However, generalizing this to a larger number of resource types is straightforward. Our framework first allows users to tune  $\tau_F$  as they would with typical hyperparameters. Once  $\tau_F$  is well-tuned, it sets  $\tau_S = \frac{1}{\alpha} \tau_F$ , where  $\alpha$  denotes the ratio of the compute power of the slower resources to that of the faster ones. The value of  $\alpha$  can be easily obtained by measuring the average training iteration time on each resource. In this study, we consider  $\alpha$  as a constant that is provided in advance. As shown in Figure 1, this system-aware adjustment of  $\tau_S$  eliminates the synchronization cost.

However, unbalanced local SGD naturally reduces the number of local updates on slower resources, which in turn slows down convergence. To address this issue, we propose introducing a well-controlled bias into local SGD training. Our framework comprises two key bias-injection methods: 1) loss-based data sampling and 2) system-aware model aggregation as described in the next subsections.

#### 4.2 Bias Injection via Data Sampling

The first key component of our framework is system-aware biased data sampling. The core idea is to allocate more important data to slower workers, thus enhancing the quality of their local models. There are several off-the-shelf bias

---

**Algorithm 1** System-aware biased local SGD framework.

---

**Require:**  $\alpha$ : the ratio of the compute power of the slower resources to that of the faster ones.,  $\lambda$ : the scaling factor for the size of the candidate data pool,  $\tau_F$ : the number of local updates per round on fast resources.

```
1:  $\tau_S \leftarrow \frac{1}{\alpha} \tau_F$ 
2: for  $t = 1 \rightarrow E$  do
3:   Randomly select  $\frac{\lambda P_S N}{P_S + \alpha P_F}$  samples.
4:    $\frac{P_S N}{P_S + \alpha P_F}$  samples with the highest losses are selected and evenly distributed among all  $P_S$  slow workers.
5:   for  $p = 1 \rightarrow P$  do
6:     if worker  $p$  is a slow worker then
7:       Locally update  $\mathbf{W}^t$  for  $\tau_S$  iterations.
8:     end if
9:     if worker  $p$  is a fast worker then
10:      Each fast worker samples  $\frac{\alpha N}{P_S + \alpha P_F}$  data.
11:      Locally update  $\mathbf{W}^t$  for  $\tau_F$  iterations.
12:    end if
13:    Record all individual loss of processed data.
14:  end for
15:   $\mathbf{W}^{t+1} \leftarrow$  Aggregate the local models,  $W_p^t$ , using Eq. (4).
16: end for
17: Return:  $\mathbf{W}^E$ 
```

---

injection methods such as simple weighted random sampling or deterministic top-k selection. We employ *power-of-d choices* method [16] to efficiently introduce bias into data sampling. More recently, the same method was used to implement biased client sampling in Federated Learning context [4].

Our biased data sampling method is described as follows.

1. **Slow workers sample candidate training data.** Given  $N$  training samples,  $\frac{\lambda P_S N}{P_S + \alpha P_F}$  samples are randomly selected without replacement, where  $P_S$  and  $P_F$  denote the number of slow and fast workers, respectively. We refer to this set as the ‘candidate data pool’. Here,  $\lambda$  is a tunable hyperparameter that controls the pool size.
2. **Slow workers select the highest-loss samples.** From the candidate data pool,  $\frac{P_S N}{P_S + \alpha P_F}$  samples with the highest loss values are selected and evenly distributed among all slow workers.
3. **Fast workers randomly sample the training data.** Each worker on faster resources independently and randomly samples  $\frac{\alpha N}{P_S + \alpha P_F}$  data without replacement.

After each worker samples its data, the slow and fast workers perform  $\tau_S$  and  $\tau_F$  local updates, respectively, using all the allocated data. Finally, the locally trained models are averaged to obtain the global model.

**Fewer but More Critical Updates on Slow Resources** — The proposed biased data sampling strategy encourages local models to focus on high-loss data samples. Since our framework allows slow workers to perform fewer updates than fast ones between synchronization points, assigning high-loss data to them enables their local models to concentrate on minimizing the corresponding loss, rather than spending effort on *easy-to-learn* samples. A similar principle has been employed in the context of random client selection in federated learning [15, 4]. In the following section, we empirically demonstrate the effectiveness of our system-aware data sampling method in heterogeneous compute environments.

### 4.3 Bias Injection via Model Aggregation

Another key component of our framework is system-aware model aggregation. Under independent and identically distributed (IID) settings, local SGD aggregates the locally trained models as follows.

$$\mathbf{W}^{t+1} = \frac{1}{P} \sum_{i=1}^P \mathbf{W}_i^t, \quad (3)$$

where  $P$  is the number of workers and  $\mathbf{W}_i^t$  is a local model trained by worker  $i$  at round  $t$ . This balanced averaging ensures that the global update is unbiased and thus minimizes the loss  $\frac{1}{N} \sum_{i=1}^N f(\mathbf{W}, \xi_i)$ , where  $N$  is the number of training samples,  $\xi_i$  is the  $i$ -th sample, and  $f(\cdot, \cdot)$  denotes the loss function. In contrast, our framework breaks this convention by assigning greater weight to more important local models.

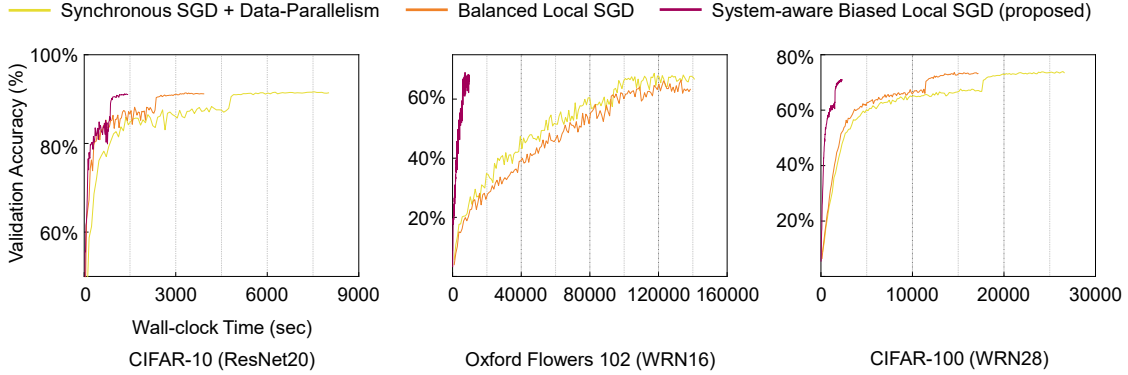


Figure 3: Learning curve comparisons. Thanks to the reduced communications and synchronization costs, our proposed method finishes the same training rounds much faster than synchronous SGD with data-parallelism and balanced local SGD.

We propose aggregating  $P$  locally trained models using the following equation.

$$\mathbf{W}^{t+1} = \sum_{i=1}^P \frac{\tau_i}{\sum_{i=1}^P \tau_i} \mathbf{W}_i^t \quad (4)$$

This aggregation method introduces bias toward local models that perform more updates. In our framework’s unbalanced local SGD setting, models trained on slower resources undergo fewer updates than those on faster ones. The key idea behind this design is to let the more extensively trained models guide the global update. By assigning greater weight to local models from faster resources, the aggregated global model becomes biased in their favor.

Note that our bias injection strategy is fundamentally opposite to the model aggregation method proposed in FedNOVA [24]. FedNOVA normalizes local updates across workers by assigning smaller weights to local models that perform more updates, thereby alleviating the ‘client drift’ issue in non-IID settings. However, our empirical study shows that this approach actually slows down convergence in IID settings. Since each worker computes stochastic gradients with the same expected value, client drift is not an issue in our case. Instead, by assigning greater weight to local models from faster resources, we are able to accelerate training.

#### 4.4 System-aware Biased Local SGD Framework

Algorithm 1 presents our biased local SGD framework. The inputs include  $\alpha$ ,  $\lambda$ , and  $\tau_F$ , which were defined and discussed earlier. At each round, slow workers (line 4 ~ 9) select their high-loss data and locally train the model for  $\tau_S$  iterations. Likewise, fast workers (line 10 ~ 13) randomly sample data and then train the model for  $\tau_F$  iterations. By parallelizing the loop at line 3, our framework effectively utilizes heterogeneous system resources. Finally, all the locally trained models are aggregated using (4) at the end of each communication round.

**Potential Limitations** – Our proposed method has two potential limitations. First, it requires slightly more memory than unbiased local SGD because the loss values of all individual training samples must be stored. However, given the size of modern neural networks, the overhead of storing a single floating-point number per sample is negligible. Second, the method involves additional computation to sort the loss values and select the highest-loss samples. Since this biased data selection is performed only once after consuming all data, the computational overhead remains minimal.

## 5 Experiments

### 5.1 Experimental Settings

**Benchmark Settings** – We evaluate our biased local SGD framework using computer vision benchmarks: CIFAR-10 [14], CIFAR-100, Oxford Flowers102 [18], and Tiny ImageNet [17], and natural language processing (NLP) benchmark: AG News [27]. For those five benchmarks, we use ResNet20 [9], Wide-ResNet28 [26], Wide-ResNet16, ViT [7], and DistillBERT [19], respectively. ViT was pretrained on ImageNet-1k [5] while DistillBERT is on Book-Corpus [1] and Wikipedia. All reported results are averaged over at least two independent runs. See Appendix for the detailed hyper-parameter settings.

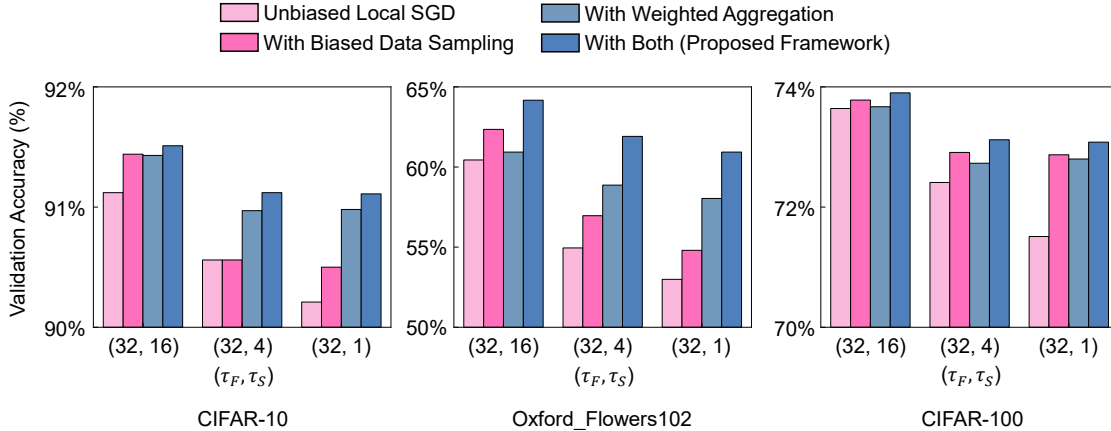


Figure 4: Model accuracy comparison with various combinations of fast and slow resources. While  $\tau_F$  is fixed at 32,  $\tau_S$  varies among 1, 4, and 16. As  $\tau_S$  decreases, meaning that the slow compute resources become slower, the accuracy of unbiased local SGD rapidly drops. As bias is introduced, the decline in accuracy is alleviated.

**System Settings** – We conduct our experiments on a GPU server equipped with two NVIDIA RTX 4090 GPUs and one AMD EPYC 7543 CPU. To simulate various CPU–GPU settings, we adjust  $\tau_S$ , which denotes the number of local updates per communication round on the slower resource. For example, given a fixed  $\tau_F = 32$ , if the slower resource has half the compute power of the faster one, we set  $\tau_S = 16$ . In our empirical study, we simulate three heterogeneous settings using  $(\tau_F, \tau_S) = (32, 16)$ ,  $(32, 4)$ , and  $(32, 1)$ .

## 5.2 Comparative Study

**Learning Curve Comparison** – We first compare our biased local SGD with synchronous SGD with data parallelism and balanced local SGD. Figure 3 shows the learning curves for three benchmarks. While all three methods achieve similar validation accuracy within the same number of updates, there is a notable difference in training time. Thanks to reduced communication frequency, balanced local SGD completes training much faster than synchronous SGD. Since model aggregation occurs every 32 local updates, its communication cost is exactly  $\frac{1}{32}$  that of synchronous SGD. However, as shown in Figure 2, balanced local SGD still suffers from synchronization overhead. Our proposed method eliminates this blocking time by adjusting  $\tau_S$  in a system-aware manner, thereby removing synchronization costs entirely. As a result, it completes training even faster than balanced local SGD.

Our unbalanced local SGD reduces  $\tau_S$  based on the performance gap between fast and slow compute resources. As a result, slow workers perform fewer updates compared to synchronous SGD or balanced local SGD, which may cause a slight drop in accuracy under the same communication round budget. However, since it completely eliminates blocking time, users can train for a few additional rounds to recover the accuracy, for instance, by running approximately 50% more rounds. In the following experiment, we evaluate how effectively the bias introduced by our proposed methods helps close the accuracy gap, enabling performance comparable to that of synchronous SGD.

**Feature-wise Comparison** – Figure 4 shows the performance comparison among four different settings: 1) unbiased local SGD, 2) local SGD with biased data sampling, 3) local SGD with weighted aggregation, and 4) local SGD with both techniques. We fix  $\tau_F = 32$  and vary  $\tau_S$  among 1, 4, and 16 to simulate different performance gaps between fast and slow compute resources. A smaller  $\tau_S$  indicates that the CPU is slower relative to the GPU. For example,  $(\tau_F = 32, \tau_S = 16)$  implies that the CPU takes twice as long as the GPU. First, as  $\tau_S$  decreases (i.e., the CPU becomes slower), unbiased local SGD suffers a sharp drop in accuracy across all three benchmarks. This degradation is primarily caused by the reduced number of updates performed by the slower worker. When bias is introduced into local training via our biased data sampling, accuracy is effectively restored. Our weighted model aggregation also leads to improved accuracy in all benchmarks. Finally, applying both techniques together results in a significant accuracy gain.

Notably, the accuracy improvements observed in Figure 4 are achieved without increasing the number of updates. Since both biased data sampling and system-aware model aggregation incur almost no additional computational cost, all four settings have nearly identical computational budgets, yet show meaningful accuracy gains. These results demonstrate that our system-aware biased local SGD is an efficient and practical optimizer for many deep learning applications.

**Performance Analysis in Various Heterogeneous System Settings** — We present additional experimental results to evaluate the proposed method under various heterogeneous system configurations. Table 1 reports results on five

Dataset	$(\tau_F, \tau_S)$	Unbiased	Biased (proposed)
CIFAR-10 (ResNet20)	(32,16)	91.12 $\pm$ 0.2%	<b>91.51</b> $\pm$ 0.3%
	(32,4)	90.56 $\pm$ 0.3%	<b>91.12</b> $\pm$ 0.1%
	(32,1)	90.21 $\pm$ 0.2%	<b>91.11</b> $\pm$ 0.1%
Oxford Flowers 102 (WRN16)	(32,16)	60.44 $\pm$ 0.8%	<b>64.17</b> $\pm$ 0.2%
	(32,4)	54.95 $\pm$ 1.1%	<b>61.91</b> $\pm$ 1.1%
	(32,1)	52.99 $\pm$ 2.2%	<b>60.93</b> $\pm$ 1.9%
CIFAR-100 (WRN28)	(32,16)	73.64 $\pm$ 0.1%	<b>73.89</b> $\pm$ 0.2%
	(32,4)	72.41 $\pm$ 0.1%	<b>73.12</b> $\pm$ 0.3%
	(32,1)	71.51 $\pm$ 0.1%	<b>73.08</b> $\pm$ 0.1%
Tiny ImageNet (ViT)	(32,16)	91.05 $\pm$ 0.1%	<b>91.43</b> $\pm$ 0.1%
	(32,4)	90.81 $\pm$ 0.1%	<b>91.39</b> $\pm$ 0.1%
	(32,1)	90.45 $\pm$ 0.1%	<b>91.38</b> $\pm$ 0.1%
AG News (DistillBERT)	(32,16)	94.11 $\pm$ 0.1%	<b>94.32</b> $\pm$ 0.1%
	(32,4)	93.93 $\pm$ 0.1%	<b>94.26</b> $\pm$ 0.1%
	(32,1)	93.84 $\pm$ 0.1%	<b>94.12</b> $\pm$ 0.1%

Table 1: Performance comparison between unbalanced local SGD (unbiased) and biased local SGD (proposed). Training runs in 1-CPU and 1-GPU setting. The  $\tau_S$  is set to 1, 4, or 16, while  $\tau_F$  is fixed to 32. Tiny ImageNet and AG News benchmarks are fine-tuning experiments.

Dataset	$(\tau_F, \tau_S)$	Unbiased	Biased (proposed)
CIFAR-10 (ResNet20)	(32,16)	91.00 $\pm$ 0.1%	<b>91.36</b> $\pm$ 0.1%
	(32,4)	90.71 $\pm$ 0.1%	<b>91.09</b> $\pm$ 0.1%
	(32,1)	90.33 $\pm$ 0.1%	<b>91.35</b> $\pm$ 0.2%
CIFAR-100 (WRN28)	(32,16)	73.74 $\pm$ 0.1%	<b>74.22</b> $\pm$ 0.1%
	(32,4)	73.64 $\pm$ 0.2%	<b>73.91</b> $\pm$ 0.1%
	(32,1)	73.22 $\pm$ 0.1%	<b>73.74</b> $\pm$ 0.1%
Tiny ImageNet (ViT)	(32,16)	91.27 $\pm$ 0.1%	<b>91.70</b> $\pm$ 0.1%
	(32,4)	91.02 $\pm$ 0.1%	<b>91.87</b> $\pm$ 0.1%
	(32,1)	90.90 $\pm$ 0.1%	<b>91.73</b> $\pm$ 0.1%
AG News (DistillBERT)	(32,16)	93.73 $\pm$ 0.1%	<b>93.95</b> $\pm$ 0.1%
	(32,4)	93.72 $\pm$ 0.1%	<b>93.91</b> $\pm$ 0.1%
	(32,1)	93.63 $\pm$ 0.1%	<b>93.87</b> $\pm$ 0.1%

Table 2: Performance comparison between unbalanced local SGD (unbiased) and biased local SGD (proposed). We simulate another case of 2-CPU and 8-GPU, the most popular settings in modern GPU servers. The  $\tau_S$  varies among 1, 4, and 16, while  $\tau_F$  is fixed to 32. Tiny ImageNet and AG News benchmarks are fine-tuning experiments.

benchmarks using 1 CPU and 1 GPU, while Table 2 presents results on four benchmarks using 2 CPUs and 8 GPUs. Note that we could not include the Oxford Flowers 102 benchmark in the 2-CPU, 8-GPU setting due to the dataset’s limited number of samples, which is insufficient to run across 10 compute resources. The Tiny ImageNet and AG News benchmarks demonstrate that our proposed framework is also readily applicable to fine-tuning scenarios.

We first observe that, across all benchmarks, unbiased local SGD suffers a non-negligible drop in accuracy as  $\tau_S$  decreases. In other words, as the performance gap between compute resources widens, the accuracy achieved within a fixed time budget declines more significantly. This trend is also evident in fine-tuning benchmarks. Second, when both types of bias, biased data sampling and weighted model aggregation, are introduced into local SGD, accuracy is effectively restored across all benchmarks. Similar improvements are observed in both the 1-CPU/1-GPU and 2-CPU/8-GPU settings. These extensive empirical results across diverse heterogeneous compute environments demonstrate that well-controlled bias can effectively accelerate local SGD and achieve higher accuracy almost without incurring additional computational cost.

SOTA	CIFAR-10	CIFAR-100	Tiny ImageNet	AG News
Balanced Averaging	90.96 $\pm$ 0.2%	72.82 $\pm$ 0.2%	91.51 $\pm$ 0.2%	93.57 $\pm$ 0.1%
FedNOVA	76.58 $\pm$ 0.1%	42.19 $\pm$ 0.3%	81.22 $\pm$ 0.1%	90.57 $\pm$ 0.3%
FedAcc	91.08 $\pm$ 0.1%	64.34 $\pm$ 0.3%	91.46 $\pm$ 0.1%	93.74 $\pm$ 0.1%
FedADP	91.20 $\pm$ 0.1%	73.51 $\pm$ 0.3%	91.43 $\pm$ 0.1%	93.75 $\pm$ 0.1%
System-aware Weighted Averaging (proposed)	<b>91.35</b> $\pm$ 0.1%	<b>73.74</b> $\pm$ 0.4%	<b>91.73</b> $\pm$ 0.1%	<b>93.87</b> $\pm$ 0.1%

Table 3: Performance comparison among different model aggregation methods. The  $(\tau_F, \tau_S) = (32, 1)$  and training runs in 2-CPU and 8-GPU setting.

$(\tau_F, \tau_S)$	$\lambda = 2$	$\lambda = 4$	$\lambda = 8$	$\lambda = 16$	$\lambda = 32$
(32, 16)	73.89 $\pm$ 0.2%	N/A	N/A	N/A	N/A
(32, 4)	72.98 $\pm$ 0.2%	73.06 $\pm$ 0.2%	73.12 $\pm$ 0.3%	N/A	N/A
(32, 1)	72.63 $\pm$ 0.1%	73.08 $\pm$ 0.1%	72.96 $\pm$ 0.1%	72.83 $\pm$ 0.1%	72.63 $\pm$ 0.1%

Table 4: Performance comparison with varying sampling ratio  $\lambda$ : CIFAR-100 (Wide-ResNet28)

### 5.3 Ablation Study

**Model Aggregation Methods** – In federated learning, it is common to determine the averaging weights based on the size of each local dataset. Our system-aware model aggregation method also assigns different weights to workers, but based on the number of local updates performed in each communication round. Therefore, we compare our method with SOTA model aggregation methods for federated learning, including FedNOVA [24], FedAcc [2], and FedADP [23]. Table 3 presents the results on four benchmarks. Interestingly, all three SOTA methods lead to a significant drop in accuracy. In contrast, our proposed aggregation method consistently outperforms balanced averaging. This observation offers an important insight: biased model aggregation methods designed for non-IID settings may be ineffective in centralized IID scenarios.

FedAcc and FedADP incur significant additional computational overhead. FedAcc assigns higher weights to local models with higher validation accuracy, requiring evaluation of all local models in every round. FedADP assigns higher weights to local models whose gradients are well aligned with the global model’s gradient, which also adds computation during aggregation. In contrast, our aggregation method introduces no such overhead, as Equation (4) is computed once  $\tau_F$  and  $\tau_S$  are specified. These results demonstrate that our proposed weighted aggregation method is more scalable than existing SOTA aggregation approaches.

**Data Sampling Ratio  $\lambda$**  – The proposed biased data sampling method has a single hyperparameter: the sampling ratio  $\lambda$ . As  $\lambda$  increases, slow workers sample a larger pool of data and then select the samples with the highest losses. Thus, a higher  $\lambda$  leads to a stronger bias toward high-loss samples. Table 4 presents the ablation results on the CIFAR-100 benchmark. Additional results on CIFAR-10 and Oxford Flowers 102 are provided in the Appendix. The cells marked as N/A indicate configurations where the sampling ratio is too large, causing the candidate pool size to exceed the total dataset size  $N$ . The best accuracy is achieved when  $2 \leq \lambda \leq 8$ . A consistent trend across other benchmarks is that  $\lambda$  should be kept sufficiently small to introduce only a mild bias toward faster workers. If  $\lambda$  is too large, the strong bias causes slow workers to repeatedly sample from a limited subset of data, which hinders effective training. Therefore, we recommend starting with  $\lambda = 2$  or 4 and tuning it further if necessary.

## 6 Conclusion

In this study, we demonstrated the potential of utilizing heterogeneous system resources, such as CPUs and GPUs, for parallel neural network training. Our extensive empirical study shows that unbalanced local SGD is a practical optimization strategy, particularly for modern GPU servers, as it eliminates costly synchronization overhead between fast and slow compute resources. Moreover, by introducing well-controlled bias into data sampling and model aggregation, unbalanced local SGD can match the accuracy of conventional synchronous SGD with data parallelism, while incurring no synchronization cost. While our study provides strong empirical evidence of the efficacy of system-aware biased local SGD, we consider understanding and further improving its theoretical performance guarantees as an important direction for future work.

## References

- [1] Jack Bandy and Nicholas Vincent. Addressing "documentation debt" in machine learning research: A retrospective datasheet for bookcorpus. *arXiv preprint arXiv:2105.05241*, 2021.
- [2] Iuliana Bejenar, Lavinia Ferariu, Carlos Pascal, and Constantin F Caruntu. Fedacc and fedaccsize: Aggregation methods for federated learning applications. In *2023 31st Mediterranean Conference on Control and Automation (MED)*, pages 593–598. IEEE, 2023.
- [3] Haw-Shiuan Chang, Erik Learned-Miller, and Andrew McCallum. Active bias: Training more accurate neural networks by emphasizing high variance samples. *Advances in Neural Information Processing Systems*, 30, 2017.
- [4] Yae Jee Cho, Jianyu Wang, and Gauri Joshi. Towards understanding biased client selection in federated learning. In *International Conference on Artificial Intelligence and Statistics*, pages 10351–10375. PMLR, 2022.
- [5] Jia Deng, Wei Dong, Richard Socher, Li-Jia Li, Kai Li, and Li Fei-Fei. Imagenet: A large-scale hierarchical image database. In *2009 IEEE conference on computer vision and pattern recognition*, pages 248–255. Ieee, 2009.
- [6] Yifan Ding, Nicholas Botzer, and Tim Weninger. Hetseq: Distributed gpu training on heterogeneous infrastructure. In *Proceedings of the AAAI Conference on Artificial Intelligence*, volume 35, pages 15432–15438, 2021.
- [7] Alexey Dosovitskiy, Lucas Beyer, Alexander Kolesnikov, Dirk Weissenborn, Xiaohua Zhai, Thomas Unterthiner, Mostafa Dehghani, Matthias Minderer, Georg Heigold, Sylvain Gelly, et al. An image is worth 16x16 words: Transformers for image recognition at scale. *arXiv preprint arXiv:2010.11929*, 2020.
- [8] Farzin Haddadpour, Mohammad Mahdi Kamani, Mehrdad Mahdavi, and Viveck Cadambe. Local sgd with periodic averaging: Tighter analysis and adaptive synchronization. *Advances in Neural Information Processing Systems*, 32, 2019.
- [9] Kaiming He, Xiangyu Zhang, Shaoqing Ren, and Jian Sun. Deep residual learning for image recognition. In *Proceedings of the IEEE conference on computer vision and pattern recognition*, pages 770–778, 2016.
- [10] Yimin Jiang, Yibo Zhu, Chang Lan, Bairen Yi, Yong Cui, and Chuanxiong Guo. A unified architecture for accelerating distributed {DNN} training in heterogeneous {GPU/CPU} clusters. In *14th USENIX Symposium on Operating Systems Design and Implementation (OSDI 20)*, pages 463–479, 2020.
- [11] Angelos Katharopoulos and François Fleuret. Not all samples are created equal: Deep learning with importance sampling. In *International conference on machine learning*, pages 2525–2534. PMLR, 2018.
- [12] Ahmed Khaled, Konstantin Mishchenko, and Peter Richtárik. Tighter theory for local sgd on identical and heterogeneous data. In *International conference on artificial intelligence and statistics*, pages 4519–4529. PMLR, 2020.
- [13] Taeyoon Kim, ChanHo Park, Mansur Mukimbekov, Heelim Hong, Minseok Kim, Ze Jin, Changdae Kim, Ji-Yong Shin, and Myeongjae Jeon. Fusionflow: Accelerating data preprocessing for machine learning with cpu-gpu cooperation. *Proceedings of the VLDB Endowment*, 17(4):863–876, 2023.
- [14] Alex Krizhevsky, Geoffrey Hinton, et al. Learning multiple layers of features from tiny images. 2009.
- [15] Fan Lai, Xiangfeng Zhu, Harsha V Madhyastha, and Mosharaf Chowdhury. Oort: Efficient federated learning via guided participant selection. In *15th {USENIX} Symposium on Operating Systems Design and Implementation ({OSDI} 21)*, pages 19–35, 2021.
- [16] Michael Mitzenmacher. The power of two choices in randomized load balancing. *IEEE Transactions on Parallel and Distributed Systems*, 12(10):1094–1104, 2002.
- [17] mnmoustafa and Mohammed Ali. Tiny imagenet. <https://kaggle.com/competitions/tiny-imagenet>, 2017. Kaggle.
- [18] Maria-Elena Nilsback and Andrew Zisserman. Automated flower classification over a large number of classes. In *2008 Sixth Indian conference on computer vision, graphics & image processing*, pages 722–729. IEEE, 2008.
- [19] Victor Sanh, Lysandre Debut, Julien Chaumond, and Thomas Wolf. Distilbert, a distilled version of bert: smaller, faster, cheaper and lighter. *arXiv preprint arXiv:1910.01108*, 2019.
- [20] Shuheng Shen, Yifei Cheng, Jingchang Liu, and Linli Xu. Stl-sgd: Speeding up local sgd with stagewise communication period. In *Proceedings of the AAAI Conference on Artificial Intelligence*, volume 35, pages 9576–9584, 2021.
- [21] Sebastian U Stich. Local sgd converges fast and communicates little. *arXiv preprint arXiv:1805.09767*, 2018.

- [22] Taegeon Um, Byungsoo Oh, Minyoung Kang, Woo-Yeon Lee, Goeun Kim, Dongseob Kim, Youngtaek Kim, Mohd Muzzammil, and Myeongjae Jeon. Metis: Fast automatic distributed training on heterogeneous {GPUs}. In *2024 USENIX Annual Technical Conference (USENIX ATC 24)*, pages 563–578, 2024.
- [23] Jiacheng Wang, Hongtao Lv, and Lei Liu. Fedadp: Unified model aggregation for federated learning with heterogeneous model architectures. In *2024 International Conference on Ubiquitous Computing and Communications (IUCC)*, pages 42–47. IEEE, 2024.
- [24] Jianyu Wang, Qinghua Liu, Hao Liang, Gauri Joshi, and H Vincent Poor. Tackling the objective inconsistency problem in heterogeneous federated optimization. *Advances in neural information processing systems*, 33:7611–7623, 2020.
- [25] Sihao Yu, Jiafeng Guo, Ruqing Zhang, Yixing Fan, Zizhen Wang, and Xueqi Cheng. A re-balancing strategy for class-imbalanced classification based on instance difficulty. In *Proceedings of the IEEE/CVF conference on computer vision and pattern recognition*, pages 70–79, 2022.
- [26] Sergey Zagoruyko and Nikos Komodakis. Wide residual networks. *arXiv preprint arXiv:1605.07146*, 2016.
- [27] Xiang Zhang, Junbo Zhao, and Yann LeCun. Character-level convolutional networks for text classification. *Advances in neural information processing systems*, 28, 2015.

## A Appendix

The appendix is structured as follows:

- Section A.1 summarizes experimental settings corresponding to all the experimental results reported in the main manuscript
- Section A.2 describes how we pre-process training and validation data.
- Section A.3 presents additional experimental results and analyses.

### A.1 Experimental Settings

To ensure reproducibility and provide a comprehensive understanding of our experimental setup, all computations were performed on a dedicated GPU server designed to simulate heterogeneous computing environments. Trainings run on a GPU server equipped with AMD EPYC 7543 CPU and two NVIDIA RTX 4090 GPUs. The system contains Ubuntu 24.04.1 LTS, Python 3.11.9, and CUDA 12.4. Our deep learning models are implemented and trained using PyTorch, with supporting libraries such as torchvision for computer vision tasks and transformers for natural language processing benchmarks. To orchestrate parallel execution across the heterogeneous compute resources (CPU and GPUs), we employ mpi4py library that enables efficient inter-process communication and synchronization in our system-aware biased local SGD framework.

**Experiments in 1-CPU and 1-GPU Setting** – For all experiments, the SGD optimizer was used. A *CosineAnnealingLR* scheduler was applied for the Tiny ImageNet dataset, while a *MultiStepLR* scheduler was used for all other datasets. Both unbalanced local SGD (unbiased) and biased local SGD (proposed) were evaluated under the same conditions as those presented in Table 5.

**Experiments in 2-CPU and 8-GPU Setting** – For all experiments, the SGD optimizer was used. A *CosineAnnealingLR* scheduler was applied for the Tiny ImageNet dataset, while a *MultiStepLR* scheduler was used for all other datasets. Both unbalanced local SGD (unbiased) and biased local SGD (proposed) were evaluated under the same conditions as those presented in Table 6.

**Fast Worker’s Number of Local Updates** – In the main manuscript, we fixed  $\tau_F = 32$  in all the experiments. The fastest compute resource in our experimental setup is the NVIDIA RTX 4090, which takes 0.1940 seconds to process a single mini-batch of CIFAR-100 using WideResNet28. In contrast, the slowest resource, the AMD EPYC 7543, requires 6.5230 seconds for the same workload. This results in a performance ratio of approximately 33 times. To reflect this worst-case performance gap, we set  $\tau_F = 32$  and  $\tau_S = 1$ .

Dataset	Batch Size	Epochs	Learning Rate	Weight Decay
CIFAR-10 (ResNet20)	64	100	0.1 (60,80 decay)	0.0001
Oxford Flowers 102 (WRN16)	32	150	0.1 (100,130 decay)	0.0001
CIFAR-100 (WRN28)	128	200	0.05 (100,180 decay)	0.0005
Tiny ImageNet (ViT)	64	10	0.0001	0.01
AG News (DistillBERT)	64	10	0.001 (7 decay)	0.0001

Table 5: Experiments in 1-CPU and 1-GPU setting.

Dataset	Batch Size	Epochs	Learning Rate	Weight Decay
CIFAR-10 (ResNet20)	32	200	0.1 (120,160 decay)	0.0001
CIFAR-100 (WRN28)	32	400	0.1 (200,360 decay)	0.0005
Tiny ImageNet (ViT)	32	20	0.0001	0.01
AG News (DistillBERT)	32	20	0.001 (14 decay)	0.0001

Table 6: Experiments in 2-CPU and 8-GPU setting.

## A.2 Data Pre-processing

**CIFAR-10 and CIFAR-100** – CIFAR datasets are preprocessed using standard data augmentation and normalization techniques commonly applied in image classification tasks. For both CIFAR-10 and CIFAR-100 datasets, the training images are randomly cropped to  $32 \times 32$  pixels with a padding of 4 pixels to add spatial variance, followed by a random horizontal flip to enhance the model’s generalization by introducing left-right variations. After these augmentation steps, all images are converted to PyTorch tensors and normalized using the dataset-specific mean and standard deviation values. The validation sets for both CIFAR-10 and CIFAR-100 undergo tensor conversion and normalization without any augmentation, ensuring a consistent evaluation protocol.

**Oxford Flowers 102** – Oxford Flowers 102 dataset is preprocessed with a series of transformations to improve model robustness and maintain consistency. Since the dataset contains more samples in ‘test’ split than ‘train’ split, we use ‘test’ split for training and others for validation. For the training data, images are first resized to  $256 \times 256$  pixels to standardize input dimensions. Then, color jitter is applied to introduce variations in brightness and contrast, followed by a random crop of  $224 \times 224$  pixels and a random horizontal flip to enhance data diversity. After these augmentation steps, the images are converted to tensors and normalized. The validation data undergo a simpler preprocessing pipeline, resizing to  $256 \times 256$ , center cropping to  $224 \times 224$ , tensor conversion, and normalization, to ensure consistent performance evaluation without augmentation bias.

**Tiny ImageNet** – Tiny ImageNet dataset is first resized to  $224 \times 224$  pixels using bicubic interpolation. For the training set, data augmentation techniques such as random horizontal flipping and *RandAugment* are applied to increase data diversity. The images are then converted to tensors and normalized using the standard ImageNet mean and standard deviation values. The validation set undergo only resizing, tensor conversion, and normalization to ensure consistent and unbiased evaluation.

**AG News** – AG News dataset is tokenized using the DistilBERT tokenizer with a maximum sequence length of 256 tokens. Then, padding and truncation are applied to ensure uniform input size. Finally, the tokenized data are formatted as PyTorch tensors with input IDs, attention masks, and labels, split into training and validation sets.

## A.3 A.3 Additional Results and Analysis

**Time-to-Accuracy Comparison** – Table 7 demonstrates the striking efficiency gain of the proposed biased Local SGD compared to the conventional Synchronous SGD with Data-Parallelism and Balanced Local SGD, particularly in terms of Wall-clock Time. This significant acceleration stems from the effective elimination of synchronization overhead, a key contribution achieved by system-aware adjustments of local update counts ( $\tau_F, \tau_S$ ) tailored to each resource’s compute capacity. While it’s observed that biased local SGD accuracy is slightly lower for the same number of epochs due to unbalanced local updates on slower resources, it completes training in a considerably shorter Wall-clock Time. Crucially, the intentionally introduced well-controlled bias through loss-based data sampling and system-aware model aggregation accelerates convergence, allowing the system to perform more communication rounds within the same time budget. This ultimately enables the achievement of comparable or even higher accuracy than synchronous SGD, but at

Dataset	Algorithm	Epochs	Accuracy	Wall-clock Time (sec)
CIFAR-10 (ResNet20)	Synchronous SGD + Data-Parallelism	100	91.62 $\pm$ 0.1%	8,025.6
	Balanced Local SGD	100	91.46 $\pm$ 0.3%	3,933.6
	System-aware Biased Local SGD (Proposed)	100	91.11 $\pm$ 0.1%	1,437.6
	System-aware Biased Local SGD (Proposed)	200	91.98 $\pm$ 0.3%	2,875.2
	System-aware Biased Local SGD (Proposed)	300	92.42 $\pm$ 0.1%	4,312.8
Oxford Flowers 102 (WRN16)	Synchronous SGD + Data-Parallelism	150	69.41 $\pm$ 0.7%	141,023.2
	Balanced Local SGD	150	65.93 $\pm$ 0.4%	138,686.9
	System-aware Biased Local SGD (Proposed)	150	60.93 $\pm$ 1.9%	5,766.0
	System-aware Biased Local SGD (Proposed)	300	73.58 $\pm$ 0.1%	11,532.1
	System-aware Biased Local SGD (Proposed)	450	79.22 $\pm$ 1.5%	17,298.1
CIFAR-100 (WRN28)	Synchronous SGD + Data-Parallelism	200	75.10 $\pm$ 0.1%	261,961.1
	Balanced Local SGD	200	74.67 $\pm$ 0.1%	254,498.3
	System-aware Biased Local SGD (Proposed)	200	73.08 $\pm$ 0.1%	7,666.9
	System-aware Biased Local SGD (Proposed)	400	75.21 $\pm$ 0.1%	15,333.8
	System-aware Biased Local SGD (Proposed)	600	75.80 $\pm$ 0.1%	23,000.7

Table 7: Performance comparison among synchronous SGD with data-parallelism, balanced local SGD, and our system-aware biased local SGD. When the epoch budget is the same, biased local SGD shows a slight decline in accuracy while dramatically reducing the training time. As our method performs more epochs, it catches up the synchronous SGD’s accuracy while still having a significantly shorter training time.

a vastly faster pace, thereby positioning biased Local SGD as a highly practical and potent solution to deep learning in heterogeneous computing environments.

**Random Sampling Scheme Comparison** – In the proposed system-aware biased Local SGD, CPU worker groups and GPU worker groups independently sample data. This design enables each worker group to access the entire dataset without restrictions, potentially allowing some data to be sampled by both groups. Under this setting, slow workers focus on learning from high-loss (challenging) data, while fast workers train on randomly sampled data. Although the slow workers perform fewer local updates, they provide important corrective signals to the global model. Meanwhile, the fast workers not only process a large volume of data through unbiased random sampling but also occasionally learn from the high-loss challenging samples. In our empirical study, we found that separating data sampling between slow and fast worker groups as described leads to more effective local SGD training, achieving the highest accuracy among all possible random sampling schemes.

Table 8 shows CIFAR-10, Oxford Flowers 102, and CIFAR-100 benchmark results obtained with three different random sampling schemes: unbiased uniform random sampling, unified random sampling, and our proposed separated sampling. The *Unified Sampling* indicates the setting where slow workers first sample the high-loss data and then fast workers randomly samples data without replacement. The *Separated Sampling* is our proposed method described in the main manuscript. As shown, our proposed *Separated Sampling* achieves the best accuracy.

The *Separated Sampling* has several benefits as follows. First, by sampling data for fast workers independently of the slow workers, their gradient estimates remain unbiased, leading to more effective training. Second, this design allows fast workers to still sample high-loss data. As a result, these challenging samples may be used in more updates, introducing a bias toward harder examples. Third, there is no synchronization points between slow and fast workers. In *Unified Sampling*, the fast workers should wait until all the slow workers finish the data sampling. Thus, it causes additional blocking points increasing the synchronization cost. For the above reasons, we argue that the proposed separated random sampling is the best design choice for efficient local SGD training.

**Performance Comparison with Varying Sampling Ratio  $\lambda$**  – To provide a more comprehensive understanding of our proposed method’s sensitivity to the sampling ratio  $\lambda$ , Table 9 and 10 present additional ablation results for the CIFAR-10 (ResNet20) and Oxford Flowers 102 (WideResNet-16) datasets, respectively. These tables show the validation accuracy achieved across varying  $\lambda$  values, while maintaining the fast resource local update count ( $\tau_F$ ) fixed at 32 and exploring different slow resource local update settings ( $\tau_S$  values of 1, 4, or 16). The N/A settings correspond to the case where the sampling size exceeds the total dataset size. We report average accuracy across at least twice independent measures.

The first observation is that the  $\lambda$  should be sufficiently small to introduce appropriate bias into data sampling process. When  $\lambda$  is too large, the candidate pool size becomes similar to the entire dataset, resulting in introducing too strong bias toward high-loss data. In contrast, when  $\lambda$  is too small, it becomes similar to the uniform random sampling. In

these two benchmarks, we observe that  $\lambda = 2$  works the best providing the highest accuracy. Therefore, we suggest beginning with  $\lambda = 2$  and carefully increasing it if needed.

Dataset	$(\tau_F, \tau_S)$	Unbiased	Unified Sampling	Separated Sampling (proposed)
CIFAR-10 (ResNet20)	(32,16)	91.12 $\pm$ 0.2%	91.25 $\pm$ 0.2%	<b>91.51</b> $\pm$ 0.3%
	(32,4)	90.56 $\pm$ 0.3%	90.87 $\pm$ 0.2%	<b>91.12</b> $\pm$ 0.1%
	(32,1)	90.21 $\pm$ 0.2%	90.89 $\pm$ 0.2%	<b>91.11</b> $\pm$ 0.1%
Oxford Flowers 102 (WRN16)	(32,16)	60.44 $\pm$ 0.8%	58.84 $\pm$ 1.3%	<b>64.17</b> $\pm$ 0.2%
	(32,4)	54.95 $\pm$ 1.1%	58.63 $\pm$ 0.6%	<b>61.91</b> $\pm$ 1.1%
	(32,1)	52.99 $\pm$ 2.2%	58.04 $\pm$ 2.8%	<b>60.93</b> $\pm$ 1.9%
CIFAR-100 (WRN28)	(32,16)	73.64 $\pm$ 0.1%	72.98 $\pm$ 0.3%	<b>73.89</b> $\pm$ 0.2%
	(32,4)	72.41 $\pm$ 0.1%	71.95 $\pm$ 0.3%	<b>73.12</b> $\pm$ 0.3%
	(32,1)	71.51 $\pm$ 0.1%	72.69 $\pm$ 0.1%	<b>73.08</b> $\pm$ 0.1%

Table 8: Performance comparison among different data sampling schemes. Training runs in 1-CPU and 1-GPU setting. The  $\tau_S$  is set to 1, 4, or 16, while  $\tau_F$  is fixed to 32.

$(\tau_F, \tau_S)$	$\lambda = 2$	$\lambda = 4$	$\lambda = 8$	$\lambda = 16$	$\lambda = 32$
(32, 16)	91.51 $\pm$ 0.3%	N/A	N/A	N/A	N/A
(32, 4)	90.87 $\pm$ 0.1%	91.12 $\pm$ 0.1%	90.96 $\pm$ 0.2%	N/A	N/A
(32, 1)	90.88 $\pm$ 0.3%	91.06 $\pm$ 0.1%	91.02 $\pm$ 0.1%	91.11 $\pm$ 0.1%	91.07 $\pm$ 0.1%

Table 9: Sampling ratio tuning : CIFAR-10

$(\tau_F, \tau_S)$	$\lambda = 2$	$\lambda = 4$	$\lambda = 8$	$\lambda = 16$	$\lambda = 32$
(32, 16)	64.17 $\pm$ 0.2%	N/A	N/A	N/A	N/A
(32, 4)	61.91 $\pm$ 1.1%	60.29 $\pm$ 0.1%	57.52 $\pm$ 1.9%	N/A	N/A
(32, 1)	60.44 $\pm$ 2.7%	58.97 $\pm$ 2.3%	58.92 $\pm$ 1.3%	55.69 $\pm$ 0.1%	60.93 $\pm$ 1.9%

Table 10: Sampling ratio tuning : Oxford Flowers 102